Engineered nanomaterials based on graphene oxide and their potentials for combined cancer therapies

Kamelia Hristova-Panusheva[1], Trayana Kamenska[1], Zlatina Gospodinova[1,2] , Natalia Krasteva[1*]

Bulgarian Academy of Science, Institute of Biophysics and Biomedical Engeneering, Sofia, Bulgaria[1]
Bulgarian Academy of Science, Institute of Plant Physiology and Genetics, Sofia, Bulgaria[2]
kamelia.t.hristova@gmail.com, trayanakamenska@abv.bg, zlatina.go@abv.bg, *natalia.krasteva@yahoo.com

Abstract: *Graphene oxide, owing to its unique physicochemical properties, has established itself as a versatile platform with applications ranging from drug delivery to medical imaging. The modification of graphene oxide has the potential to enhance crucial properties such as near-infrared (NIR) adsorption capacity, water dispersity, and cytotoxicity. This paper aims to discuss the potential of unmodified graphene oxide and polyethylene glycol (PEG)-modified graphene oxide nanoparticles as responsive systems to NIR in the context of combined photothermal and chemotherapy. The focus is on their application for treating colorectal and hepatocellular cancer cells, highlighting their promise in integrated cancer therapies.*

Keywords*: MODIFIED GRAPHENE OXIDE, PEGYLATED GRAPHENE OXIDE, PHOTOTERAPIES, CHEMOTHERAPY, COLON 26 CELLS, HEPG2 CELLS*

1. Introduction

Engineered nanomaterials (ENMs) have recently garnered significant attention for many applications, ranging from optoelectronic, electronic, cosmetic, dental bonding, and imaging to drug delivery systems [1-3]. The central focus is on certain nanomaterials like graphene oxide (GO), an oxidized form of graphene, known for its cost-effectiveness, abundance, and ease of processing [4-6]. The interest in GO is immense and comes from its unique one-atom thin sheet structure [7, 8], which ensures a high specific surface area with de-localized electrons, facilitating efficient drug loading. The heightened interest in GO is further attributed to its high content of oxygen-containing functional groups. These groups located on the edge or basal planes of the GO sheets offer high reactivity and can be easily modified for biomolecule attachment. The modifications improve the physicochemical properties of GO, such as NIR adsorption capacity, water dispersity, and drug loading/delivery capacity [9, 10]. Current literature supports that PEGylation is pivotal in mitigating the cytotoxicity of various graphene oxide derivatives while enhancing their physiological stability and pharmacokinetic properties [11-13]. Notably, GO-PEG serves a dual purpose as a photosensitizer (photothermal absorbent) in photothermal therapy (PTT) and as a drug carrier. This dual functionality positions GO-PEG as a promising candidate for the development of intelligent nanoplatforms, offering synergistic anti-cancer therapies [14].

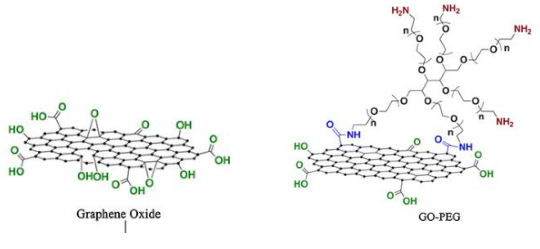

Fig. 1. *Schematic illustration of graphene oxide(GO)and PEGylated graphene oxide (GO-PEG)*

Consequently, we have subjected graphene oxide (GO) nanoparticles to modification using polyethylene glycol (PEG) and evaluated their biological efficacy against two different cancer cell lines: HepG2, representing hepatocellular cancer, and Colon26, representative of colorectal cancer. This evaluation was conducted following near-infrared (NIR) irradiation.

2. Experimentals

2.1 Synthesis of GOs nanoparticles

The synthesis of nano-graphene oxide (nGO) and nGO-PEG nanoparticles (NPs) followed a well-established protocol, as detailed previously [14-16]. In brief, a water solution containing GO (Graphenea, Spain) at a concentration of 1 mg/ml underwent sonication for 2 hrs at 500 W (VCX 500, Sonics and Materials, Inc., Newtown, CT, USA) in order to achieve nanosized GO.

For the preparation of nGO-PEG NPs, mPEG-NH2 (Abbexa Ltd., Cambridge, UK) was added to nGO solution. The resulting mixture was sonicated at the same conditions for 5 min and was subsequently incubated for 22 hrs in a water bath at 70^0 C. The resultant nGO-PEG was centrifuged to remove unbounded PEG and was then stored at 4^0 C.

2.2. Physico-chemical characterization of GOs Nanoparticles

The average size, size distributoion and zeta potential of the nanoparticles were characterized by Zetasizer, following a previously described methodology [14].

2.3. Cell culture

The mouse colorectal cancer cell line, Colon 26 and HepG2, a hepatocellular cancer cell line, were purchased from American Tissue Culture Collection (ATCC) and was maintained in DMEM medium supplemented with 10% foetal calf serum and antibiotic/antimicotic solution at 37°C in a fully humidified atmosphere at 5% CO_2.

2.4 Assessment of biological activity of GOs nanoparticles

The cells were seeded at a density of $1x10^4$ cell in 96-well plates for cell viability assessment, $1x10^4$ cell in 24-well plate for overall cell morphology evaluation, and $1x10^5$ cell in 6-well plates for cell motility assessment. The cells were allowed to incubated for 24 hrs before exposure to nanoparticles with a concentration of 100 μg/ml. At the next day the cells underwent irradiation for 5 or 15 minutes at 808 nm depending on the cell culture plate, and were subsequently stained with fluorescein diacetate (FDA) to evaluate the alteration in cell morphology as previously described [15].

Cell viability after 24 hours of incubation with nanoparticles was assessed using the WST-1 kit from Takara, following the manufacturers' instructions. For the evaluation of cell motility, a wound healing assay was conducted at the 24-hour of incubation of cells with NPs coupled with a 5 minute laser irradiation at 808 nm.

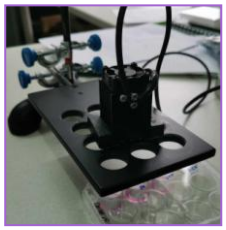

Fig. 2. *A single 808 nm near-infrared light (NIR) laser system used for irradiation of cancer cells*

2.5. Statistical analysis

The data presented in this article are expressed as means ± standard deviation (SD). Statistical differences between groups were determined using analysis of variance (ANOVA), and probability levels of 0.05 and 0.01 were considered to indicate statistical significance.

3. Results and Discussion

3.1. Physico-chemical properties of GOs nanoparticles

Zetasizer measurements revealed that the unmodified graphene oxide (GO) NPs exhibited a negative charge, characterized by a zeta potential value of -32.9 mV, and an average particle size of 252.7 nm (as shown in Table 1). Conversely, upon PEGylation GO NPs displayed increased dimensions of 324.6 nm, accompanied by a reduced negative charge of -21.6 mV. The observed size variations in both types of GO nanoparticles are attributed to the introduction of a larger PEG moiety (0.35 kDa). Additionally, the substitution of the negatively charged -COOH group in GO molecules with neutral PEG molecules probably contributed to the decrease in negative zeta potential

Table 1. *Zeta potential and average particle size of GO and GO-PEG NPs in water solution*

Type of NPs	Surface charge [mV]	Average particle size [nm]
nGO	-32.9	252.7
nGO-PEG	-21.6	324

The particle size distribution analysis indicated an increase after PEGylation, with the size distribution of nanographene oxide (nGO) particles ranging from 43.82 nm to 458.7 nm. In contrast, nGO-PEG particles exhibited a broader size range from 164.2 nm to 615.1 nm. This observation suggests that the PEGylation process led to a dispersion of sizes in the graphene oxide nanoparticles, contributing to a broader range in the distribution of particle sizes.

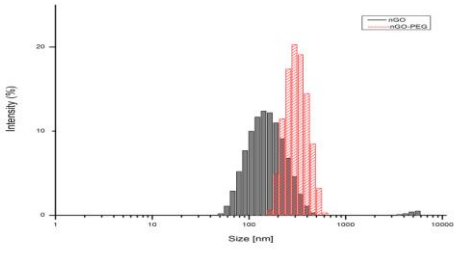

Fig. 3. *Particle size distribution of nGO and nGO-PEG NPs*

3.2. Biological activity of GOs Nanoparticles

The FDA staining and WST-1 assay results (see Fig.3 and Fig.4) illustrated a distinct impact of both nanoparticles, alone and in conjunction with near-infrared (NIR) irradiation, on both cell lines. In Colon 26 cells, NIR irradiation suppressed the viability of untreated and graphene oxide (GO)-treated Colon 26 cells but stimulates viability in cells treated with GO-PEG. Conversely, a slight stimulation of cell viability was observed after irradiation of control and GO-treated HepG2 cells while no noticeable effect was observed in GO-PEG-treated cells. These findings highlight the differential responses of Colon 26 and HepG2 cells to the combined influence of NPs and NIR irradiation.

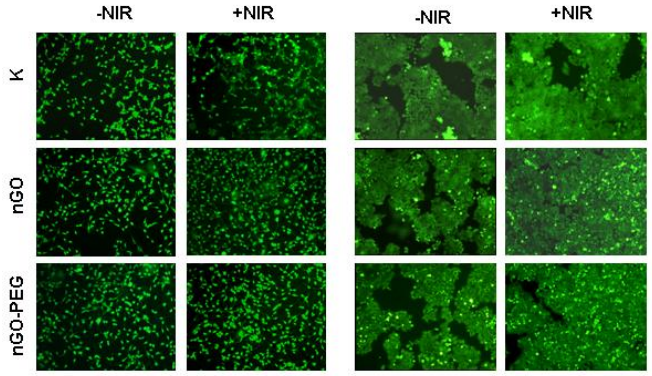

Fig. 4. *FDA micrographs of Colon 26 cells (left panel) and HepG2 cells (right panel) incubated for 24 hrs with nGO and nGO-PEG NPs, and irradiated for 5 min at 808 nm; magnification 10x*

An intriguing observation is that in Colon 26 cells the synergic effect of both types of GO nanoparticles and NIR irradiation closely resembles the impact observed in irradiated controls. In contrast, in HepG2 cells, the most significant inhibitory effect on cell viability was observed in non-irradiated GO-treated cells. This suggests cell-type-specific responses, indicating that the combined influence of GO and NIR irradiation may vary in its effectiveness across different cancer cell lines. Understanding these distinct responses is crucial for tailoring nanoparticle-based therapies for specific cancer types.

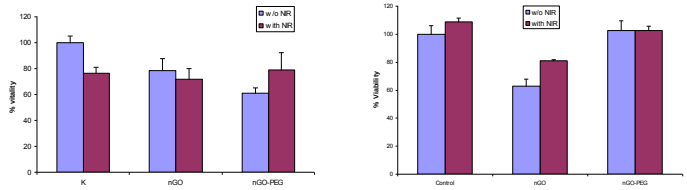

Fig. 5. *Viability of Colon 26 cells (left) and HepG2 cells (right) after 24 hrs incubation with nGO and nGO-PEG NPs, followed by 5 min irradiation with 808 nm*

Recognizing the crucial role of cellular migration in tumor invasion and metastasis [16], our objective was to investigate the impact of nGO and nGO-PEG, with and without near-infrared irradiation, on cell migration using the *in vitro* wound-healing assay. Both cell lines were exposed to 100 µg/mL of nGO and nGO-PEG, incubated for 24 hrs and then subjected to 15 minutes of NIR irradiation with 808 nm. The results depicted in Fig. 5. showed the effects on cancer cell migratory capacity resulting from nanoparticle treatment alone and in combination with NIR irradiation, with evaluations conducted 24 hours after cellular incubation.

Upon assessing the combined effects of nanoparticles (NPs) and near-infrared (NIR) irradiation on Colon26 motility, the most pronounced inhibitory effect was observed in cells treated with nGO-PEG and subjected to NIR irradiation. In the case of HepG2

cells, the analysis of wound healing results unveiled a more robust inhibitory effect of both NPs compared to the untreated control.

These findings underscore the differential impact of NPs and NIR irradiation on the motility of Colon26 and HepG2 cells, emphasizing the importance of considering cell-type-specific responses in therapeutic applications.

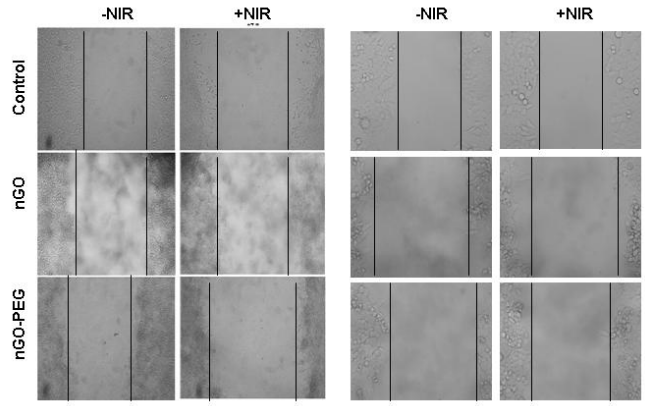

Fig. 5. *Wound closure of Colon 26 cells (left panel) and HepG2 cells (right panel), after 24 hrs incubation with nGO and nGO-PEG NPs, followed by 15 min irradiation with 808 nm, magnification 10x*

4. Conclusions

In summary, our findings indicate that unmodified (nGO) and PEGylated nano-graphene oxide (nGO-PEG) nanoparticles exhibit varying potential for cancer treatment, depending on the specific type of cancer cells under consideration. The differential responses observed underscore the importance of tailoring nanoparticle-based therapies according to different cancer cell types' distinct characteristics and behaviors. This insight contributes to a nuanced understanding of the applicability and effectiveness of nGO nanoparticles in the context of cancer treatment strategies.

5. Acknowledgements

This work was supported by a grant from the National Scientific Fund of Bulgaria, project No KP-06 N31/15 from 2019. Research equipment of Distributed Research Infrastructure INFRAMAT, part of Bulgarian National Roadmap for Research Infrastructures, 2020-2027, supported by the Bulgarian Ministry of Education and Science, was used in this investigation.

6. References

1. V. Gubala, L. Johnston, Z. Liu, H. Krug, C.J. Moor, Ch.K. Ober, M. Schwenk, M. Vert, Pure Appl. Chem. 90, 8 (2018)
2. C. Tomuleasa, O. Soritau, A. Orza, M. Dudea, B. Petrushev, O. Mosteanu et al, J. Gastrointestin. Liver Dis. 21 (2012)
3. K. Hadinoto, A. Sundaresan, W.S. Cheow, Eur. J. Pharm. Biopharm. 85 (2013)
4. A. K. Geim, K. S. Novoselov, Nat Mater, 6, 3 (2007)
5. S. Guo, S. Dong, Chem. Soc. Rev. 40, (2011)
6. D. P. Singh, C. E. Herrera, B. Singh, S. Singh, R. Singh, R. Kumar, Mater. Sci. Eng. 86, (2018)
7. G. Yang, L. Li, W.B. Lee, M.C. Ng, Sci Technol Adv Mater. 19, 1 (2018)
8. F. Kim, L.J. Cote, J Huang, Adv. Mater. 22 (2010)
9. X. Tan, L. Feng, J. Zhang, K. Yang, S. Zhang, Z. Liu, R. Peng, ACS Appl. Mater. Inter.5 (2013)
10. J. Zhang, X. Lu, C. Shi, B. Yan, L. Gong, J. Chen, L. Xiang, H. Xu, Q. Liu, H. Zeng, Chem. Eng. J. 358 (2019)
11. T. Kamenska, M. Abrashev, M. Georgieva, N. Krasteva, Materials (Basel), 14, 17 (2021)
12. X. Pei, Z. Zhu, Z. Gan, J. Chen, X. Zhang, X. Cheng, Q. Wan, J. Wang. Sci Rep. 10, 1 (2020)
13. A. Sasidharan, L.S. Panchakarla, P. Chandran, D. Menon, S. Nair, C.N.R. Rao, M. Koyakutty. Nanoscale, 3 (2011)
14. N. Krasteva, D. Staneva, B. Vasileva, G. Miloshev, M. Georgieva, Nanomaterials (Basel).11, 11 (2021)
15. M. Georgieva, Z. Gospodinova, M. Keremidarska-Markova, T. Kamenska, G. Gencheva, N. Krasteva, Pharmaceutics. 13, (2021)
16. Z. Gospodinova, T. Kamenska, G. Gencheva, M. Georgieva, N. Krasteva, J. Phys. Conf. Ser. (2021)